

Non-uniform Surface Impedance Absorbing Boundary Condition for FDTD Method

Yunlong Mao¹, Atef Z. Elsherbeni², Si Li¹, and Tao Jiang¹

¹Department of Information and Communication Engineering
Harbin Engineering University, Harbin, Heilongjiang, 150001, China
maoyunlong@hrbeu.edu.cn, lisiharbin@hrbeu.edu.cn, jiangtao@hrbeu.edu.cn

²Department of Electrical and Computer Engineering
Colorado School of Mines, Golden, CO, 80401, USA
aelsherb@mines.edu

Abstract — Recently, we reported a novel absorbing boundary condition (ABC), surface impedance absorbing boundary (SIABC). SIABC has a comparable absorbing performance compared to CPML, but requires a sufficient long distance between the boundary and the scatter. In this paper, we focus on this issue and introduce the non-uniform SIABC. Non-uniform SIABC archives a similar absorbing performance as the uniform SIABC at a same distance, while the number of the air buffer cells is much smaller. Therefore, it is possible for us to make it more efficient relative to uniform SIABC or CPML. An example of a patch antenna is discussed to explore the accuracy and efficiency of non-uniform SIABC. We also compare the memory usage for uniform SIABC, non-uniform SIABC, and 10-layers CPML. All the results indicate that non-uniform SIABC requires much less memory, needs much less time for simulations, which makes it a potential of being one of the most popular ABCs in FDTD method.

Index Terms — CPML, FDTD, Non-uniform, SIABC.

I. INTRODUCTION

Surface impedance absorbing boundary condition is first introduced by us in [1]. SIABC comes from the concept of surface impedance boundary condition (SIBC) proposed by Leontovich in 1940s [2]. It is implemented by setting the impedance the same as free space. Compared to CPML [3], SIABC is extremely easy for understanding and for programming, meanwhile, it has a comparable absorbing performance relative to 10 layers CPML. Despite of these advantages, the disadvantage of SIABC is also obvious. In order to absorb the incident waves efficiently, a sufficient long distance between SIABC and the scatter is always required. Therefore, the memory requirement enlarges with the increase of number of air buffer cells. In some situations, this increase may

be significant.

On the purpose of reducing the memory usage, we propose the non-uniform SIABC. Non-uniform gridding is a good way to reduce the simulation time with an acceptable accuracy. Non-uniform gridding is proposed originally to deal with complex geometrically details by changing large grids into smaller grids. However, for non-uniform SIABC, the general purpose of non-uniform gridding is inverted. We build larger grids for the air buffer between the boundaries and the scattering objects, in order to reduce the number of air buffer cells. There are a few non-uniform methods proposed [4-6], and in this paper, we will apply the gradually changing grid method as described in [7].

In the first section of this paper, we briefly described non-uniform sub-gridding and how it is combined with SIABC method. Later, we test the accuracy and efficiency of non-uniform SIABC with a microstrip antenna example. The results are compared with 8-layers CPML and show a good agreement. The memory requirements are also compared to 10-layers CPML for general simulations. It can be concluded that non-uniform SIABC is an excellent ABC, and has the potential of being one of the most popular ABCs in FDTD method.

II. NON-UNIFORM FORMATTING

The geometrical illustration of grid discretization of non-uniform grid SIABC is displayed in Fig. 1 [7].

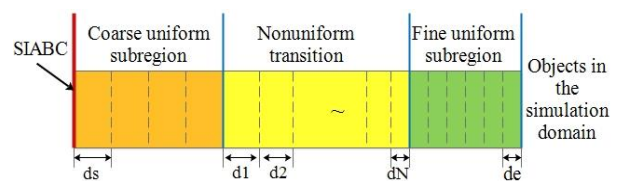


Fig. 1. Geometrical illustration of non-uniform SIABC.

In Fig. 1, the air buffer between the SIABC boundary and the objects inside the simulation domain is divided into 3 sub-regions: coarse uniform sub-region, non-uniform transition sub-region, and fine uniform sub-region. The objects in the simulation domain are located in the fine uniform sub-region. In the coarse uniform sub-region, the cell size is ds ; in the non-uniform transition sub-region, the cell size changes from ds to de gradually with the same decreasing ratio, and in the fine uniform sub-region, the cell size is de . The length of the first cell in the transition sub-region is set as:

$$d1 = Rds, \quad (1)$$

where R is the ratio of change between subsequent half cells. In the transition sub-region, the length of each cell is changing gradually, hence, the length of each cell in the transition sub-region can be represented as:

$$dM = R^M ds, \quad (2)$$

where M is the index of the M th cell in the transition sub-region. At the beginning of the fine uniform sub-region, the length of the fine cells should be:

$$de = R^{N+1} ds, \quad (3)$$

where N is the number of the cells in the transition sub-region. If the transition is desired to happen on a given length ΔT , the total length of the transition sub-region, in addition to one cell at both ends from the uniform regions is:

$$\Delta T + ds + de = \sum_{k=0}^{N+1} dsR^k = \frac{ds - deR}{1 - R}. \quad (4)$$

Therefore, ratio R can be calculated as:

$$R = \frac{\Delta T + de}{\Delta T + ds}. \quad (5)$$

Then, the number of cells, N , can be determined using:

$$N = \frac{\log(de/ds)}{\log(R)} - 1. \quad (6)$$

One should notice that N must be an integer number. It can be rounded to its closest appropriate integer. A smoother transition can be archived if the transition sub-region is selected to be appropriately long.

Another important thing is that the size of the coarse grid should be chosen properly. As is known to all, the larger the coarse grid is, the smaller number of air buffer cells there will be. However, larger grid will cause instability during the simulation [8-10]. Therefore, a proper selection of coarse grids will reduce the cells needed meanwhile keep the stability of the simulation. As time duration is determined by the fine grids, there is no need to consider it separately.

The format of updating equations for non-uniform SIABC are totally the same as those of uniform SIABC method, while the cell size, dx , dy and dz , should be replaced with coarse grids.

III. VERIFICATION EXAMPLES

A. Microstrip patch antenna

In this example, a patch antenna as described in [7] is used to examine the performance of non-uniform SIABC. A microstrip rectangular patch antenna is constructed, as shown in Fig. 2. The problem domain is identified with grid size $\Delta x=2$ mm, $\Delta y=2$ mm, $\Delta z=0.95$ mm, which are regarded as fine grids in this example. A rectangular brick represents the substrate of the antenna with $60\text{mm} \times 40\text{mm} \times 1.9\text{mm}$ dimension and 2.2 dielectric constant. A PEC plate for the ground of the antenna is placed at the bottom side of the substrate covering its entire surface area. A PEC patch is centered on the top surface of the substrate with 56 mm width and 20 mm length in the x and y directions, respectively. The feeding point to the top patch is at the center of the long edge of the patch. A voltage source with 50 internal resistance between the ground plane and the feeding point is defined. This patch antenna operates at 3.45 GHz. The simulation with 8-layers CPML, uniform SIABC and non-uniform SIABC are employed in turn. In each simulation, the number of time steps is 8000. These simulations are executed on a personal computer operating with Inter(R) Core(TM) i7-4700MQ, running at 2.4 GHz.

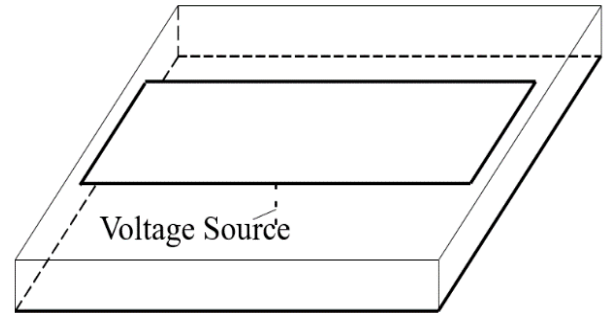


Fig. 2. A microstrip patch antenna configuration.

The performance of non-uniform SIABC is compared to uniform SIABC and 8-layers CPML. For the CPML case, the number of air buffer cells is 10. For the uniform SIABC case, the number of air buffer cells is 20. For the non-uniform SIABC cases, the number of air buffer is 20 and 30. The coarse grid is 5 mm in x and y directions, and 2.85 mm in z direction. The transition length is 21 mm in x and y directions and 8.55 mm in z direction. There are 2 fine grids before the transition region starts. A domain size comparison (in terms of number of cells) of 8-layers CPML, uniform SIABC, and non-uniform SIABC is shown in Table 1 along with the required CPU time. The comparison of the power reflection coefficient is shown in Fig. 3.

Table 1: Comparison of CPML, uniform SIABC and non-uniform SIABC in dimension size and simulation time

ABCs	$n_x \times n_y \times n_z$	Domain Size	CPU Time (m)
CPML-8	$66 \times 56 \times 38$	140,448	8.01
SIABC-uniform	$70 \times 60 \times 42$	176,400	7.98
SIABC-non 20	$52 \times 42 \times 22$	48,048	1.35
SIABC-non 30	$60 \times 50 \times 26$	78,000	2.22

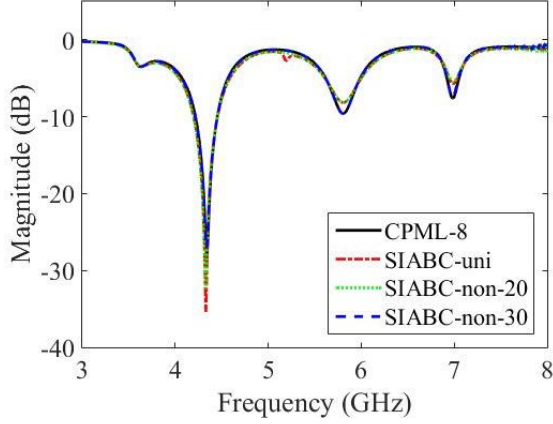


Fig. 3. Comparison of 8-layers CPML, uniform SIABC and non-uniform SIABC for power reflection coefficient.

From Table 1 and Fig. 3, one can figure out that compared to uniform SIABC or 8-layers CPML, non-uniform SIABC requires much less memory storage, and needs much less time for the simulation with the same reflection coefficient performance. For this example, the domain size for non-uniform SIABC is almost half of that for 8-layers CPML, while the time needed for the simulation is just around 1 fourth. That is because from the complexity aspect, SIABC is much easier than CPML.

B. Memory comparison

In this section, we compare the memory storage requirement for 10-layers CPML, uniform SIABC with its number of air buffer cells ranging from 20 to 50, and non-uniform SIABC with the same air buffer length as uniform SIABC has. Due to the fact that for non-uniform SIABC, the coarse grids will vary with different problems, we made an assumption that for all situations, the coarse grid is three times of the fine grid, and the transition length between coarse sub-region and fine sub-region is 3 times of a coarse grid. Also, there are 2 fine grids in front of the scattering object. Therefore, ratio R can be calculated as:

$$R = \frac{\Delta T + de}{\Delta T + ds} = \frac{9ds + ds}{9ds + 3ds} = \frac{5}{6}, \quad (7)$$

and the number of cells in the transition sub-region, N , should be:

$$N = \frac{\log(de/ds)}{\log(R)} - 1 = 5.0. \quad (8)$$

The air buffer gridding is illustrated in Fig. 4. There are 20 fine grids for uniform SIABC case and correspondingly, there are 10 cells for non-uniform SIABC case. There are 3 coarse grids and 2 fine grids. The other 5 cells comes from the transition sub-region, with their cell size decreasing from ds to de .

In order to reduce the number of cells for a certain length, the number of coarse grids should be as many as possible. In our discussion, as the number for fine grids is settled down, we should adjust the length of transition sub-region to ensure that we can have as many coarse grids as possible. Table 2 shows the number of air buffer cells comparison for uniform SIABC and non-uniform SIABC. In the first column, we list the number of air buffer cells for uniform SIABC, which is changing from 20 to 50. The rest of the columns list the corresponding number of cells for non-uniform SIABC: the number of coarse cells, the length for transition length in terms of de , the number of cells for the transition sub-region, N , the number of cells in the fine region, and the total number of cells used.

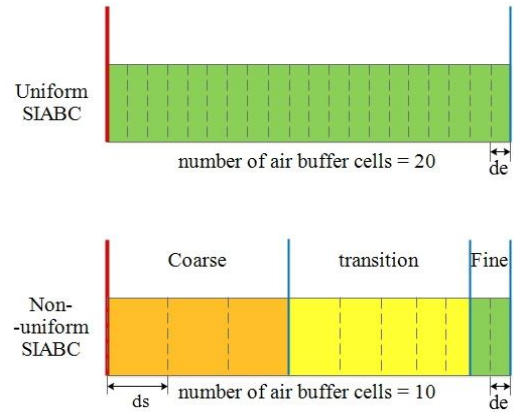


Fig. 4. Air buffer cells configurations for uniform SIABC and non-uniform SIABC with fixed air buffer length.

Table 2: Number of air buffer cells comparison

Uniform (cells)	Non-uniform (cells)				
	Coarse	Transition Length (de)	N	Fine	Total
20	3	9	5	2	10
30	6	10	6	2	14
40	9	11	6	2	17
50	13	9	5	2	21

The memory comparison result is shown in Fig. 5. Generally speaking, by using non-uniform SIABC, the memory requirement is significantly smaller than 10-

layers CPML, especially for problems with small domain size.

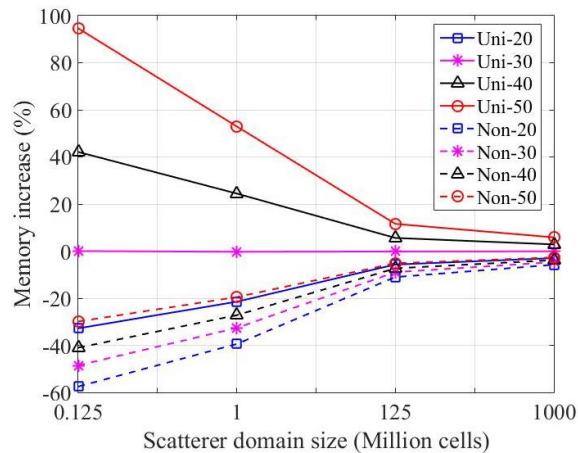


Fig. 5. Memory increase relative to 10-layers CPML.

IV. CONCLUSION

In this paper, an advanced absorbing boundary condition, non-uniform SIABC is proposed which is a combination of non-uniform grid and SIABC. By applying non-uniform grid, we significantly reduced the number of air buffer cells between the SIABC boundaries and the scattering objects leading to much smaller memory requirements relative to uniform SIABC or CPML with acceptable accuracy. Hence, non-uniform SIABC has the potential of being one of the most easy to implement with good performance and less memory requirements ABC for electromagnetic simulations.

REFERENCES

- [1] Y. Mao, A. Z. Elsherbeni, S. Li, and T. Jiang, "Surface impedance absorbing boundary for terminating FDTD simulations," *Applied Computational Electromagnetics Society Journal*, vol. 29, pp. 1035-1046, 2014.
- [2] M. Leontovich, "Approximate boundary conditions for the electromagnetic field on the surface of a good conductor," *Investigations on Radiowave Propagation*, vol. 2, pp. 5-12, 1948.
- [3] J. A. Roden and S. D. Gedney, "Convolutional PML (CPML): An efficient FDTD implementation of the CFS-PML for arbitrary media," *Microwave and Optical Technology Letters*, vol. 27, pp. 334-338, 2000.
- [4] S. S. Zivanovic, K. S. Yee, and K. K. Mei, "A subgridding method for the time-domain finite-difference method to solve Maxwell's equations," *Microwave Theory and Techniques, IEEE Transactions on*, vol. 39, pp. 471-479, 1991.
- [5] P. Thoma and T. Weiland, "A consistent subgridding scheme for the finite difference time domain method," *International Journal of Numerical Modelling: Electronic Networks, Devices and Fields*, vol. 9, pp. 359-374, 1996.
- [6] K. Xiao, D. J. Pommerenke, and J. L. Drewniak, "A three-dimensional FDTD subgridding algorithm with separated temporal and spatial interfaces and related stability analysis," *IEEE Transactions on Antennas & Propagation*, vol. 55, pp. 1981-1990, 2007.
- [7] A. Z. Elsherbeni and V. Demir, *The Finite-difference Time-domain Method for Electromagnetics with MATLAB® Simulations*. 2nd ed., Edison, NJ: SciTech Publishing, an Imprint of the IET, 2016.
- [8] J. S. Juntunen and T. D. Tsiboukis, "Reduction of numerical dispersion in FDTD method through artificial anisotropy," *IEEE Transactions on Microwave Theory & Techniques*, vol. 48, pp. 582-588, 2000.
- [9] T. Martin and L. Pettersson, "Dispersion compensation for Huygens' sources and far-zone transformation in FDTD," *IEEE Transactions on Antennas & Propagation*, vol. 48, pp. 494-501, 2000.
- [10] J. B. Schneider and R. J. Kruhlak, "Dispersion of homogeneous and inhomogeneous waves in the Yee finite-difference time-domain grid," *IEEE Transactions on Microwave Theory & Techniques*, vol. 49, pp. 280-287, 2001.
- [11] J. H. Beggs, R. J. Luebbers, K. S. Yee, and K. S. Kunz, "Finite-difference time-domain implementation of surface impedance boundary conditions," *Antennas and Propagation, IEEE Transactions on*, vol. 40, pp. 49-56, 1992.